Can the MaxFlux algorithm describe bifurcating paths?

ARTICLE *in* THEORETICAL CHEMISTRY ACCOUNTS · OCTOBER 2007

Impact Factor: 2.23 · DOI: 10.1007/s00214-007-0290-x · Source: OAI

2 AUTHORS, INCLUDING:

Ramon Crehuet
Spanish National Research Council
46 PUBLICATIONS **686** CITATIONS

SEE PROFILE

Theor Chem Account (2007) 118:769–775
DOI 10.1007/s00214-007-0290-x

REGULAR ARTICLE

Can the MaxFlux algorithm describe bifurcating paths?

A comparison with analytic and Transition Path Sampling results

Aurora Jiménez · Ramon Crehuet

Received: 5 December 2006 / Accepted: 27 March 2007 / Published online: 16 June 2007

Abstract Temperature-dependent reaction paths have been calculated with the MaxFlux algorithm for a bifurcating region of the potential energy surface of the blocked alanine dipeptide. The resulting paths agree with an ensemble of trajectories generated with Transition Path sampling, which has also been used to determine product distributions. The Valley Ridge Inflection point has been shown to lie close to the point of maximum curvature of the MaxFlux paths.

1 Introduction

The traditional view that transition states (TS) connect reactant and product minima along the minimum energy path (MEP) has been challenged recently by both experimental and theoretical investigations [1–7]. Unexpected product distributions obtained for some systems, can be understood assuming there is a branching of the reaction paths after the transition state, which leads to two different minima. This implies a departure from the MEP. Of course, the MEP has only a physical meaning in its asymptotic interpretation: it is the path followed by a molecule when the temperature tends to zero and the friction to infinity [8,9]. For real systems these conditions are not met and deviations from the MEP occur. Whether we call these deviations "dynamical" is a matter of nomenclature. They are dynamical in the sense that they arise from thermal movement present at any non-zero temperature, but they need not be inertial effects, i.e., they can appear in Newtonian, Langevin or Brownian models, as we will show, which are systems that evolve under very different dynamical equations. Thus, we will refer to the deviations of the MEP as temperature effects.

The branching of a reaction valley often occurs when a TS with high symmetry leads to products with lower symmetry [5,6]. In such a case, the MEP from the TS connects with a TS with the same symmetry, and this TS connects the two lower symmetry products. In other words, the transition vector of the later TS belongs to the the non-symmetric irreducible representation of its point group. These systems have been thoroughly studied and there exist several methods to locate branching points and calculate product distributions, even classical TST can be applied [10]. To apply these methods, one follows the MEP calculating (or updating) the Hessian matrix at each point until one finds a Valley-Ridge inflection point (VRI). A VRI is defined as the point where the gradient is orthogonal to an eigenvector of the Hessian with null eigenvalue [11,12]. After this point, the approximation of the PES as a harmonic well for this eigenvalue breaks down, but TST can still be applied to get product distributions (which only have a meaning when one has isotopically differentiated molecules) [10].

It is worth pointing out that the name 'minimum energy path' is not rigorously appropriate after the VRI, where it becomes a *maximum* energy path for the negative eigenvalue. Indeed, it would be more correct to talk about the steepest descent line from the TS—and this is the definition we are using—as the MEP is not uniquely defined after the VRI [13]. A detailed analysis of the behaviour of the MEP at a VRI has been recently discussed by Bofill et al. [14]. Remark that, using this definition the VRI is a one-dimensional geometrical object [12].

Unfortunately the picture of a MEP passing through a VRI will break down for molecules without symmetry even if the reaction path remains quasi-symmetric. Under these circumstances the MEP will avoid the VRI. According to

A. Jiménez · R. Crehuet (✉)
IIQAB–CSIC, Jordi Girona 18–26, 08034 Barcelona, Spain
e-mail: rcsqtc@iiqab.csic.es

[7], "no qualitative theory presently exists for understanding selectivity in such reactions, and trajectory calculations are required for quantitative predictions". Sampling is done by throwing trajectories from the TS and counting the product distribution [1,7,15]. An even more general approach can be based on transition path sampling (TPS). This method does not require the definition of a transition state and gives an equilibrium ensemble of reactive trajectories. It is further described in the following section.

To overcome the problem that arises in the lack of symmetry, a more general definition of a VRI has been given by Quapp [12]. This alternative VRI (hereafter a Q-VRI) is the intersection with the IRC of the hypersurface with a direction of zero curvature perpendicular to the gradient. This borderline is defined as

$$\mathbf{g}^T \mathbf{H}_{\text{adj}} \mathbf{g} = 0 \tag{1}$$

where $\mathbf{H}_{\text{adj}}$ is the adjoint of the Hessian $\mathbf{H}$. The main difference with the standard definition is that the gradient need not be an eigenvector of the Hessian because the direction with zero curvature can be a combination of the adjoint Hessian eigenvectors with non-zero eigenvalues. Thus all VRI's are Q-VRI's but not vice-versa. We will comment on the utility of this definition in the next section.

In this letter we propose and test the use of the MaxFlux method, based on the Smoluchowski equation, to find possible bifurcations and product distributions and we introduce the concept of using TPS to calculate product distributions. We compare the MaxFlux results with exact results from TPS and give a statistical interpretation of the MaxFlux path. The comparison with the topological analysis of the PES based on Eq. (1) shows that it can be used to locate bifurcating regions. The paper is distributed as follows. In Sect. 2, we give a description of the theoretical basis, implementation and description of a test molecular system; and in the Sect. 3, we explore its applicability to that molecular system under different dynamics.

To the knowledge of the authors this is the only method that can account for reaction branching without having to sample trajectories or calculating Hessian matrices, and thus, at a much lower cost. In this sense it can be seen as an extension of the MEP that can override some of its limitations for branching reactions.

2 Methods

The MaxFlux path is based upon work by Berkowitz et al. [16] who derived variational formulas for the optimum path, assuming that the system obeys the Smoluchowski equation. The Smoluchowski equation is the over-damped limit of the Fokker–Plank equation, the equation that governs the evolution of a system under the influence of both stochastic and deterministic forces.

Starting from the Smoluchowski equation, Berkowitz et al. showed that the flux of particles, $\mathbf{j}$, along an optimal reaction path, $\mathcal{P}$, satisfies

$$\begin{aligned}\int_{\mathcal{P}} \mathrm{d}\boldsymbol{s} \cdot \mathbf{j}\gamma \exp(\beta U) &= -k_B T \int_{\mathcal{P}} \mathrm{d}\boldsymbol{s} \cdot \nabla \left(P(t)\exp(\beta U)\right) \\ &= -k_B T \left[P(t)\exp(\beta U)\right]_A^B\end{aligned} \tag{2}$$

This equation assumes that an optimal path exists along which all particles will flow and that the friction coefficient, γ, is a constant, independent of particle positions. In this equation, s is the coordinate describing the position along the path, U is the potential energy of the system and $\beta = 1/k_{\text{B}}T$ where k_{B} is the Boltzmann constant and T is the temperature. Under stationary conditions the flux can be considered a constant. We can assume an absorbing boundary at B which is equivalent to consider only the positive flux from A to B. Under this circumstances, the flux is independent of the potential in B:

$$j_{A\to B} = \frac{1}{\beta\gamma} \frac{P(A)\exp(-\beta U(A))}{\int_A^B \exp(\beta U)\mathrm{d}s} \tag{3}$$

This equation allows us to compare different fluxes for different paths provided they have the same reactant point A. This integral equation has an associated differential Euler-Lagrange equation which has a simpler interpretation:

$$\kappa\hat{\mathbf{n}} + \hat{\mathbf{t}}(\beta\nabla U \cdot \hat{\mathbf{t}}) - \nabla\beta U = 0 \tag{4}$$

where κ is the curvature of the path, and $\hat{\mathbf{n}}$ and $\hat{\mathbf{t}}$ are the principal unit vectors normal and tangent to the path, respectively. The key is that the perpendicular component of the gradient ($\mathbf{g} = \nabla U$) is not zero as in the MEP but:

$$\mathbf{g}_\perp = \frac{\kappa}{\beta}\hat{\mathbf{n}} \tag{5}$$

So that the temperature tends to favour straight (less curvature) paths and allows for deviations of the MEP. Indeed, at 0 K the most probable path is the MEP, as shown by Olender and Elber [8].

There are different ways to implement this algorithm as described in [17,18]. We have used the implementation described in [18], which is based on a nudged-elastic-band description of the path [19]. The implementation was done in the DYNAMO molecular simulation library [20]. A similar approach but based on the path-integral formalism of the transition probability was used by Elber [8,21] and Soskin [22]

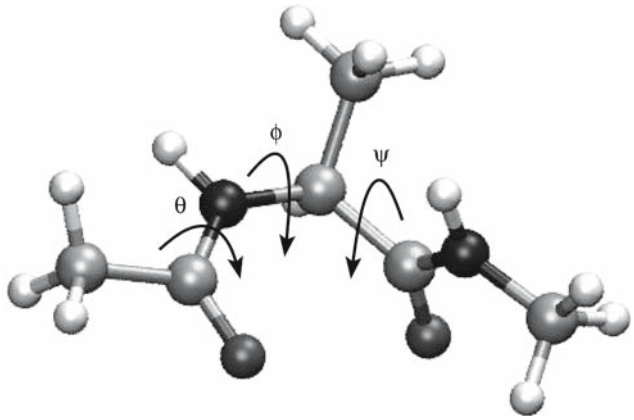

Fig. 1 Ball-and-sticks representation of the blocked alanine dipeptide (CH_3–CONH–$CHCH_3$–CONH–CH_3) and the angles used in this work

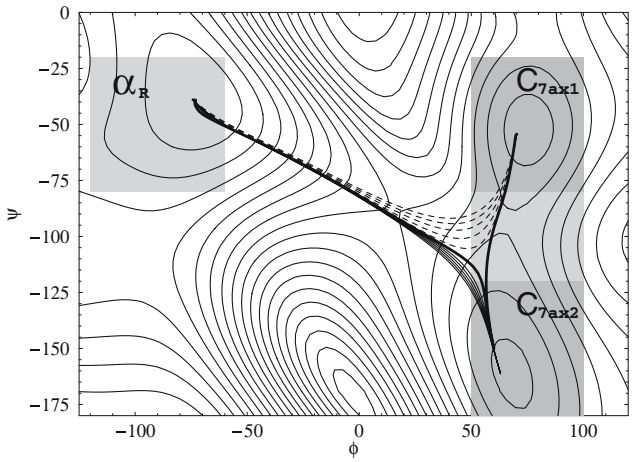

Fig. 2 Potential energy surface of the bALA with the MEP path (*bold*), the MaxFlux paths that go to C_{7ax1} (*dashed*), and to C_{7ax2} (*solid*). MaxFlux paths are printed for the following temperatures: 200, 300, 400, 500 and 600 K. The area used to define the reactants and product regions is also shown as *shaded rectangles*. *Light gray rectangles* define the reactant and product regions used in the TPS and the *two dark grey rectangles* define the two product regions used for the product distribution analysis of the TPS trajectories

to give a (more complex) expression for the most probable path.

The system used for this work is the alanine dipeptide, aka blocked alanine (see Fig. 1). The description of this system has been thoroughly tackled by Apostolakis et al. [23] and has also been used as a test for TPS calculations [24] and other dynamical studies [25,26]. In our previous work [18] we found that the temperature-dependent paths on this system show a significant departure from the MEP. The main variables to describe this molecule are the dihedral angles ϕ and ψ. It was pointed out in [24,26] that θ is also relevant for the kinetics. In this paper we will focus on the conformational change between the conformations α_R and C_{7ax}, which are described below. The system was studied in solution with a Generalized Born/Surface Area model (GBSA) [27,28]. The potential energy was described by the OPLS-AA force field [29]. The MaxFlux paths were optimised at 200, 300, 400, 500 and 600 K. Each path was discretised in 101 structures.

Transition Path Sampling (TPS) was developed with the aim of giving rate constants for which the choice of a reaction coordinate is complex. In its essence it generates an equilibrium ensemble of reactive trajectories as a first step and then, in a second step, calculates the weight of this ensemble with respect to all trajectories, which finally gives the rate constant. This second step is the most time consuming. We will make use of the first step to generate an ensemble of trajectories and will analyse the distribution of products that takes place when the reaction path branches. TPS is a purely dynamical method in the sense that does not make use of the dividing surface needed for all TS theories. It can be implemented for Newtonian, Langevin or Brownian dynamics, as described in [30]. TPS in these three variants was also implemented in the DYNAMO library [20,31]. The basins for the reactant α_R and the products C_{7ax1} and C_{7ax2} are defined in Fig. 2.[1] The products include both basins for product C_{7ax1} and C_{7ax2}. After the TPS procedure the ensemble of trajectories was analysed to get the product distribution between C_{7ax1} and C_{7ax2}. The use of TPS for product distributions is a novelty of this work and has the advantage that it is much less expensive than rate calculations.

We have performed TPS with different kind of dynamics: Langevin with three different friction coefficient($\gamma = 0.5, 5, 10\,\mathrm{ps}^{-1}$) and Brownian ($\Delta t/\gamma = 5 \times 10^{-6}\,\mathrm{ps}^2$). TPS was modified to include each kind of dynamics. A total of 1,000 uncorrelated trajectories were generated on each case. The duration of the event is 1,740 steps of 0.5 fs for Langevin Dynamics and 3,960 steps for Brownian Dynamics.

Transition Path Sampling works with a fixed trajectory time and this time should be large enough to accommodate all the distribution of time lapses since a molecule leaves the reactant basin until it gets to the product basin. This duration depends a lot on the temperature and less on the friction. For low temperatures and large γ the trajectory length was too short; we have discarded this results which correspond to the missing points in Fig. 3.

3 Results and discussion

When studying the transitions between the minima α_R and C_{7ax1} in Ref. [18] we found a interesting result. The TS

[1] The GBSA-OPLS combination that we have used here and in [18] splits C_{7ax} into two different minima which we have labelled C_{7ax1} and C_{7ax2}.

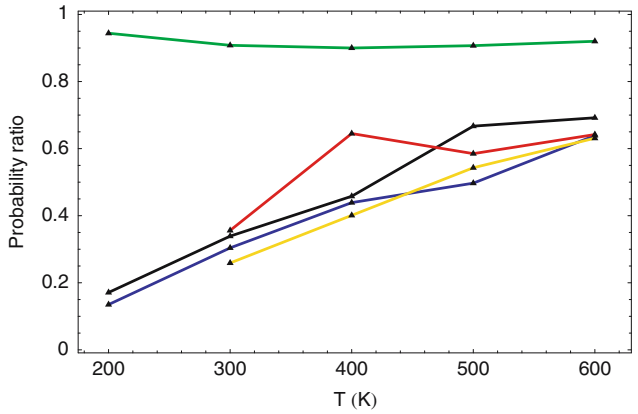

Fig. 3 Ratio of probabilities to go to C_{7ax1} over probabilities to go to C_{7ax2}. MaxFlux (green), Langevin, $\gamma = 0.5$ (*black*), $\gamma = 5$ (*blue*), $\gamma = 10$ (*yellow*), and Brownian (*red*)

located at $\phi \sim 10$ connected α_R with C_{7ax2}, while no TS could be found connecting α_R with C_{7ax1}. However, the MaxFlux path curved away from the MEP and connected directly α_R with C_{7ax1}, avoiding the minimum C_{7ax2}. (Fig. 2) As expected, higher temperatures give paths with less curvature and with a larger departure from the MEP. The temperature effects are more important for paths going to C_{7ax1}. As we will see below, this is related to the existence of a VRI in that region.

Transition Path Sampling product distribution is shown in Fig. 3. As the temperature grows, the product ratio becomes closer to one, as expected. It is also remarkable the fact that the friction coefficient has an almost negligible effect. This small dependence on the external friction shows that the reaction path is mainly coupled to the other internal degrees of freedom so that the energy transfer for this process is mainly intramolecular [32]. Brownian dynamics are close to low-friction Langevin results, showing also that inertial effects do not play any role along this reaction path. This is in contrast to other chemical processes such as the ones described in [1,33]. This is probably due to the fact that the amplitude of the conformational change studied in this work has a much larger amplitude than bond forming processes in [1, 33]. Remembering that the MaxFlux is based on an overdamped description of the movement along the reaction path, the process in this work is suited for the study with MaxFlux.

The results for the product ratio with MaxFlux are also plotted in Fig. 3. We can see that MaxFlux correctly favours product C_{7ax2} over product C_{7ax1}, however the quantitative results disagree. In all the cases the flux differences are far too small. The reason for this is the flux value is mainly determined by the energy at the top of the barrier, as can be seen in Eq. (3), whereas the bifurcation of the path takes place at lower energies. We have to remember that the main dependence of flux is on the temperature. At 200, 400, and 600 K the fluxes to C_{7ax1} (in arbitrary units) are 7.3×10^{-6}, 1.3×10^{-3}, 6.7×10^{-3}, respectively. The difference between fluxes to C_{7ax1} and C_{7ax2} are much smaller and the effect of the bifurcation is not quantitatively captured in the coarse approximation done for the MaxFlux simplification. Indeed, the product distribution depends mainly on the shape of the PES when deviating from the MEP, and to get an analiytic relatively accurate description of this region one needs, at least, the Hessian matrix.

But even though the MaxFlux results do not give quantitative product distributions they can give other valuable insight such as the position of the bifurcation. We can extend the Q-VRI definition to include MaxFlux paths by stating that a Q-VRI will take place for any given path that crosses the region defined by Eq. (1). Of course we want to retain the simplicity of our approach, so that we want to avoid the calculation of Hessian matrices which are necessary for the exact location of the Q-VRI. But can we estimate its position? With the help of Eq. (5) we can see that the points with largest gradient component perpendicular to the path will be the ones with largest curvature. These will be the paths that are furthest away from the MEP. Figure 4 shows that this is indeed the case for bALA. Figure 4 shows the regions where there is a Q-VRI. The points located from the maximum curvature lie relatively close to this region in agreement with our hypothesis that maximum departure from the MEP will take place where the region is flat, i.e. the Hessian eigenvalue parallel to the curvature of the path is small. In other words, Eq. (5) tells us that the r.h.s. term tends to make paths straight until it is compensated by the gradient, and in a flat region the gradient increases slowlier when we depart from the MEP, so that larger departures are needed to fulfill Eq. (5). Of course, the theory underlying the VRI and the MEP lacks the concept of temperature and, although it can be given a dynamical picture [34], the

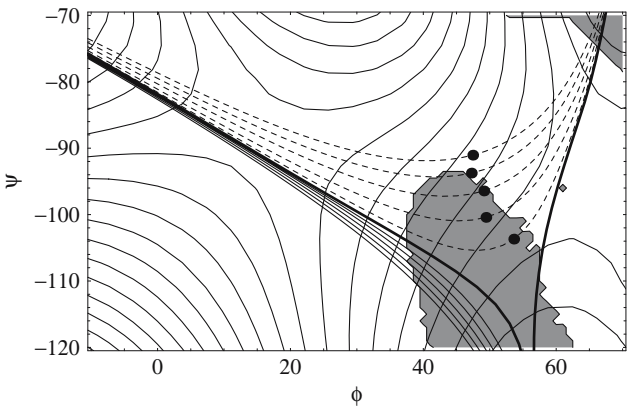

Fig. 4 Regions where $\mathbf{g}^T \mathbf{H}_{adj} \mathbf{g}$ is negative (*white*) and positive (*grey*). The points with maximum curvature of the MaxFlux paths (*black dots*) lie close to the region where there is the sign change

dynamical equations are different from the Smoluchowski equation that underlies the MaxFlux algorithm. The agreement between both formalisms shows that they are describing the same physical situation. The advantage of the MaxFlux is that the Hessian matrix is never calculated.

We can further analyse the points of maximum curvature (PMC) to check if they are turning points (TP). TP are defined as points where the tangent of the path and the gradient are orthogonal [35]. Equation (5) could suggest that PMC will also be TP but this equation only considers the perpedicular component of the gradient. If the slope of the PES is high, the parallel component will be large and the tangent and the gradient will never become completely orthogonal. This is what happens at all but the lowest temperature, but at 200 K there is a TP and it corresponds to the PMC, as is represented in Fig. 5.

Now we turn to a statistical analysis of the paths. If a potential were symmetric in the direction perpendicular to the MEP and if there were no inertial effects, a given point on the MEP would represent the average distribution of molecules for the plane perpendicular to the path at that point. When a potential, such as the one is this work, breaks the symmetry, the average position of molecules that go to the minima will be different. The analysis of the projection of the trajectories generated with TPS on the $\psi - \phi$ angles show the average paths followed by the molecules. These average paths are similar to the transition tubes defined by Vanden-Eijnden, which can also be calculated with his finite-temperature string method, in the case they are sufficiently localised [25,36]. Figure 6 shows that the TPS analysis on product distributions is valid, as there is not a significant number of transitions going between C_{7ax1} and C_{7ax2}. Once a molecule gets to one of the product basins, it remains there. Therefore, the populations that we measure do not correspond to thermodynamic averages between C_{7ax1} and C_{7ax2}, but to kinetic product distributions. These distributions arise because of the bifurcation. The MaxFlux path correctly follows the regions of highest density of transition trajectories, both for C_{7ax1} and C_{7ax2}. It can be interpreted as the average path of the ensemble of trajectories,

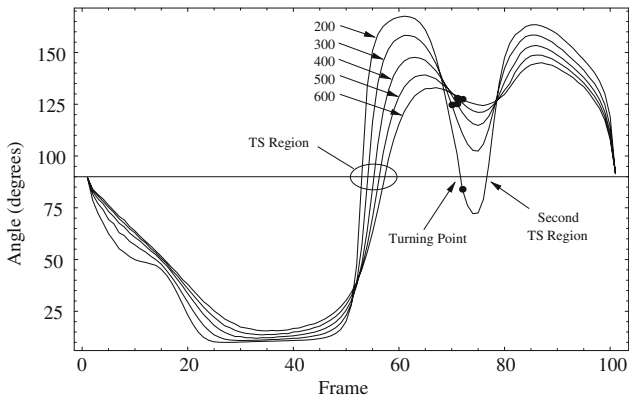

Fig. 5 Angle formed between the gradient and the tangent. The first turning point corresponds to the TS region at $\phi \sim 20$. The second TS is located at $\phi \sim 65$. The PMC's are marked as *dots*. For all but the lowest temperature the paths go continuously downhill from the first TS to the C_{7ax1} region without a TP. For the path at 200 K, the PMC and the TP nicely agree (the small disagreement arises from the discretisation of the path)

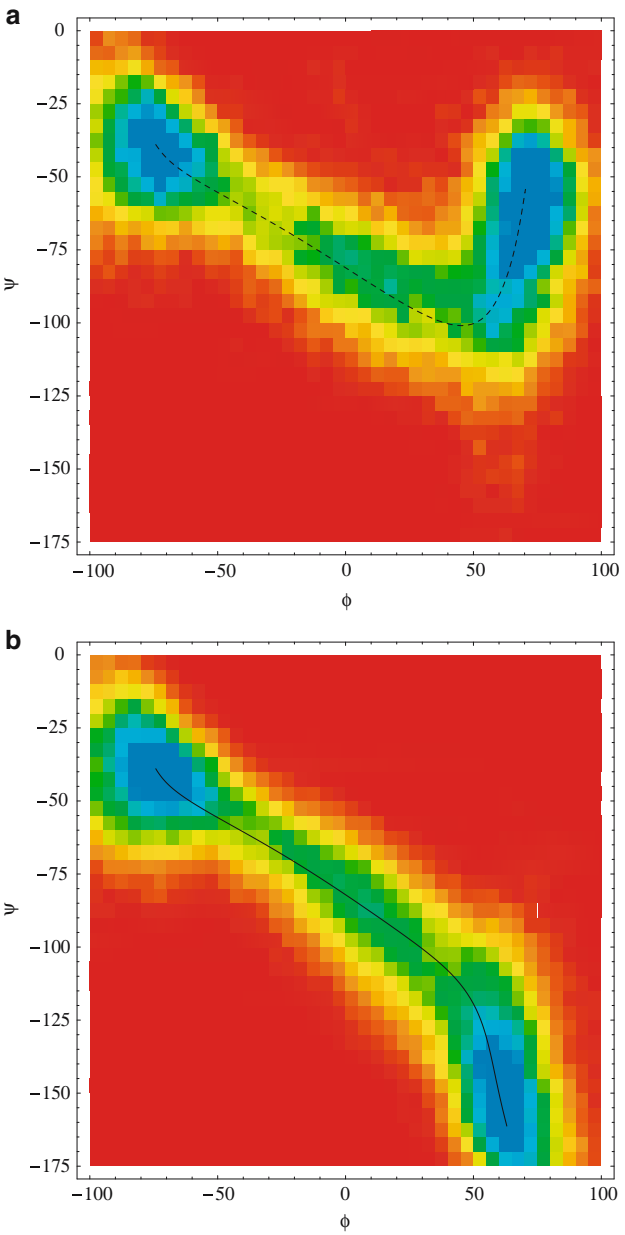

Fig. 6 Density of molecules from the TPS trajectories (T = 300 K, γ = 10 ps^{-1}) that go to C_{7ax1} in (**a**) and to C_{7ax2} in (**b**). The colour range is red-green-blue from low to high. MaxFlux paths at 300 K are overimposed

as an extension of the MEP, which fails for bifurcating mechanisms.[2]

4 Conclusions

In this work we have shown how TPS can be used to obtain product distributions at a much lower cost than rate constants. We have also seen that the MaxFlux path can account for path bifurcations, but cannot reproduce the quantitative results of TPS. It can locate, at a much lower costs, regions where bifurcations of the reaction path occur and can give temperature dependent average paths. A possible future work will be to implement reaction path Hamiltonians [37,38] onto this path to get more insight of energy flows along the path.

Acknowledgments We acknowledge J.M. Anglada for helpful suggestions. R.C. Would like to thank the Ramón y Cajal programme and A.J. the CSIC and the European Social Fund for her I3P fellowship. We also acknowledge financial support from the Spanish Drección General de Investigación científica y Técnica (Grant CTQ2006-01345/BQU) and by the Generalitat de Catalunya (Grant 2005SGR00111). Some of the calculations were performed at the CESCA, which we also acknowledge.

References

1. Carpenter BK (1998) Dynamic behaviour of organic reactive intermediates. Angew Che Int Ed 37:3340
2. Bartsch RA, Chae YM, Ham S, Birney DM (2001) Experimental and theoretical studies on the thermal decomposition of heterocyclic nitrosamines. J Am Chem Soc 123(31):7479
3. Zhou C, Birney DM (2002) Sequential transition states and the valley–ridge inflection point in the formation of semibullvalene. Org Lett 4(19):3279
4. Carpenter BK (2005) Nonstatistical dynamics in thermal reactions of polyatomic molecules. Annu Rev Phys Chem 56:57
5. Lasorne B, Dive G, Desouter-Lecompte M (2005) Wave packets in a bifurcating region of an energy landscape: Diels-Alder dimerisation of cyclopentadiene. J Chem Phys 122:184304
6. Doubleday C, Suhrada CP, Houk KN (2006) Dynamics of the degenerate rearrangement of bicyclo[3.1.0]hex-2-ene. J Am Chem Soc 128:90
7. Ussing BR, Hang C, Singleton DA (2006) Dynamic effects on the periselectivity, rate, isotope effects, and mechanism of cycloadditions of ketenes with cyclopentadiene. J Am Chem Soc 128:7594
8. Olender R, Elber R (1997) Yet another look at the steepest descent path. J Mol Struct THEOCHEM 398–399:63
9. Vanden-Eijnden E (2006) Transition path theory. In: Ferrario M, Ciccotti G, Binder K (eds). Computer simulations in condensed matter: from materials to chemical biology, vol. 1 1st edn. Lecture Notes in Physics vol 703. Springer, Berlin
10. González-Lafont A, Moreno M, Lluch JM (2004) Variational transition state theory as a tool to determine kinetic selectivity in reactions involving a valley-ridge inflection point. J Am Chem Soc 126(40):13089
11. Valtazanos P, Ruedenberg K (1986) Bifurcations and transition states. Theor Chim Acta 69:281
12. Quapp W, Hirsch M, Heidrich D (2004) An approach to reaction path branching using valley-ridge inflection points of potential energy surfaces. Theor Chem Acc 112:40
13. Hirsch M, Quapp W (2004) Reaction pathways and convexity of the potential energy surface: application of Newton trajectories. J Math Chem 36:307
14. Aguilar-Mogas A, Crehuet R, Giménez X, Bofill JM (2007) Applications of analytic and geometry concepts of the theory of calculus of variations to the intrinsic reaction coordinate model. (submitted to Mol Phys)
15. Bakken V, Danovich D, Shaik S, Schlegel HB (2001) A single transition state serves two mechanisms: an ab initio classical trajectory study of the electron transfer and substitution mechanisms in reactions of ketyl radical anions with alkyl halides. J Am Chem Soc 123:130
16. Berkowitz M, Morgan JD, McCammon JD, Northrup SH (1983) Diffusion-controlled reactions: A variational formula for the optimum reaction coordinate. J Chem Phys 79(11):5563
17. Huo S, Straub JE (1997) The MaxFlux algorithm for calculating variationally optimized reaction paths for conformational transitions in many body systems at a finite temperature. J Chem Phys 107(13):5000
18. Crehuet R, Field MJ (2003) A temperature-dependent nudged-elastic-band algorithm. J Chem Phys 118:9563
19. Jónsson H, Mills G, Jacobsen KW (1998) Nudged elastic band method for finding minimum energy paths of transitions. In: Berne BJ, Ciccotti G, Coker DF (eds) Classical and quantum dynamics in condensed phase simulations. World Scientific, Singapore, pp 385–404
20. Field MJ, Albe M, Bret C, Proust-de Martin F, Thomas A (2000) The DYNAMO library for molecular simulations using hybrid quantum mechanical and molecular mechanical potentials. J Comput Chem 21(12):1088
21. Elber R, Shalloway D (2000) Temperature dependent reaction coordinates. J Chem Phys 112(13):5539
22. Soskin SM (2006) Most probable transition path in an overdamped system for a finite transition time. Phys Lett A 353:281
23. Apostolakis J, Ferrara P, Caflisch A (1999) Calculation of conformational transitions and barriers in solvated systems: application to the alanine dipeptide in water. J Chem Phys 110(4):2099
24. Bolhuis PG, Dellago C, Chandler D (2000) Reaction coordinates of biomolecular isomerization. Proc Nat Acad Sci 97(11): 5877
25. Ren W, Vanden-Eijnden E, Maragakis P, E W (2005) Transition pathways in complex systems: application of the finite-temperature string method to the alanine dipeptide. J Chem Phys 123:134109
26. Maragliano L, Fischer A, Vanden-Eijnden E, Ciccotti G (2006) String method in collective variables: minimum free energy paths and isocommittor surfaces. J Chem Phys 125:024106
27. Still WC, Tempczyk A, Hawley RC, Hendrickson T (1990) Semianalytical treatment of solvation for molecular mechanics and dynamics. J Am Chem Soc 112:6127
28. Qiu D, Shenkin PS, Hollinger FP, Still WC (1997) The GB/SA continuum model for solvation. A fast analytical method for the calculation of approximate Born radii. J Phys Chem A 101: 3005
29. Jorgensen WL, Maxwell DS, Tirado-Rives J (1996) Development and testing of the OPLS all-atom force field on conformational energetics and properties of organic liquids. J Am Chem Soc 118:11225
30. Dellago C, Bolhuis PG, Geissler PL (2002) Transition path sampling. Adv Chem Phys 123:1

[2] We have also checked θ values at the transition region, which are relevant to define the TS as discussed in [18,24,26], but they show no significant difference between both paths.

31. Crehuet R, Field MJ (2006) A transition path sampling study of the reaction catalyzed by the enzyme chorismate mutase. J Phys Chem B (in press). doi:10.1021/jp067629u
32. Gershinsky G, Berne BJ (1999) The dependence of the rate constant for isomerisation on the competition between intramolecular vibrational relaxation and energy transfer to the bath: a stochastic model. J Chem Phys 110:1053
33. Nummela JA, Carpenter BK (2002) Nonstatistical dynamics in deep potential wells: a quasiclassical trajectory study of methyl loss from the acetone radical cation. J Am Chem Soc 124(29):8512
34. Crehuet R, Bofill JM (2005) The reaction path intrinsic reaction coordinate method and the Hamilton–Jacobi theory. J Chem Phys 122:234105
35. Quapp W (2001) Comment on the quadratic reaction path evaluated in a reduced potential energy surface model and the problem to locate transition states (by J. M. Anglada, E. Besalú, J. M. Bofill, and R. Crehuet, J Comput Chem 2001, 22, 4, 387–406). J Comput Chem 22(5):537
36. E W, Ren W, Vanden-Eijnden E (2005) Finite temperature string method for the study of rare events. J Phys Chem B 109:6688
37. Miller WH, Handy NC, Adams JE (1980) Reaction path hamiltonian for polyatomic molecules. J Chem Phys 72(1):99
38. González J, Giménez X, Bofill JM (2001) On the reaction path hamiltonian for polyatomic molecules. J Phys Chem A 105(20):5022